# Understanding chiral crossings with local and global symmetry constraints

Moritz M. Hirschmann
Max Planck Institute for Solid State Research, Germany
November 10, 2022

# Topological band crossings

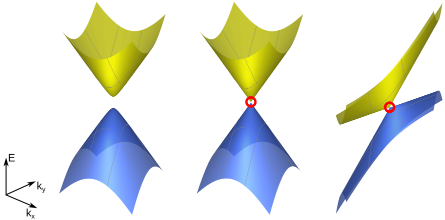


Two-fold screw rotation $\tilde{C}_2^z$

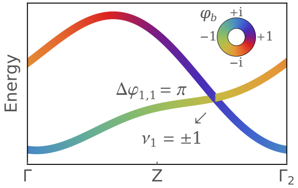


Implications of band crossings

- Top. invariants
  Chern number, chirality
- Surface states
- Effects on transport properties

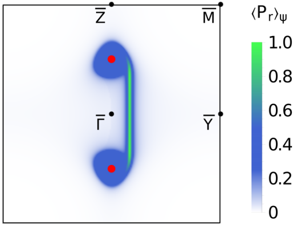

# Symmetries relate Weyl points

Symmetry $D$ on chirality $\nu_{\mathbf{k}}$

- Rotations and time reversal: $\nu_{\mathbf{k}} = \nu_{D\mathbf{k}}$
- Mirror and Inversion: $\nu_{\mathbf{k}} = -\nu_{D\mathbf{k}}$

Yet, time reversal $\not\Rightarrow$ four Weyl points.

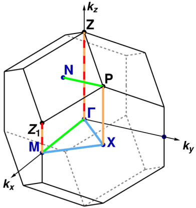


three Weyl points

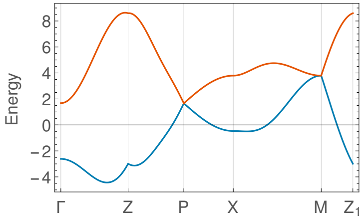


SG 80 ($I4_1$) spinless

two Weyl points

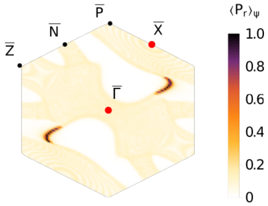


SG 119 ($I\bar{4}m2$) spinful

**Hirschmann, M. M.**, Leonhardt, A., Kilic, B., Fabini, D. H., Schnyder, A. P. (2021). *Physical Review Materials, 5(5), 054202.*

# Outline

1. Local constraint

   Relation between rotation eigenvalues and the chirality

2. Global constraint

   Enforced band exchange by (non)symmorphic symmetry

3. Applications of global and global constraints

   Double Weyl points in TaAs

   Quasi-symmetry-protected quadruple Weyl points

   Fourfold crossing with Chern number $\nu = 5$

   Topological nodal planes

   Chiral nodal lines

# Local constraint I

Consider Weyl points:

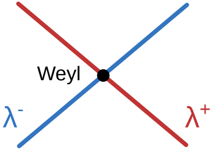


- rotation symmetry $C_n$
- eigenvalues $C_n \left| E_b \right\rangle = \lambda_b \left| E_b \right\rangle$ for band index $b$
- crossing between rotation eigenvalues $\lambda_b^+$ and $\lambda_b^-$

Goal: Determine the Chern number $\nu$ using $\Delta\varphi_b = \varphi_b^+ - \varphi_b^-$ with $\varphi_b^{\pm} = \arg\lambda_b^{\pm}$.

1. Chern number $\nu$ = Integral of Berry curvature
2. Rotation symmetry $C_n$ simplifies the integration.

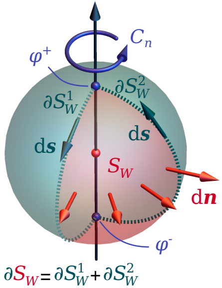

# Local constraint II

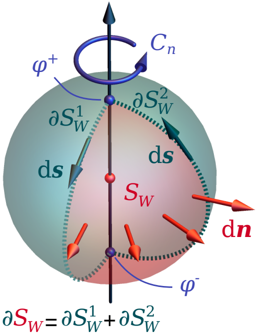


3. Apply Stokes theorem
4. Symmetry-related paths partially cancel
5. At the north and south pole the phase $\Phi(\boldsymbol{k})$ reduces to $\varphi^\pm$

$$\begin{aligned}
\nu &= \frac{n}{2\pi} \int_{S_W} \mathrm{d}\boldsymbol{n} \cdot \boldsymbol{\Omega}(\boldsymbol{k}) \\
&= \frac{n}{2\pi} \left( \int_{\partial S_W^1} \mathrm{d}\boldsymbol{s} \cdot \boldsymbol{A}(\boldsymbol{k}) + \int_{\partial S_W^2} \mathrm{d}\boldsymbol{s} \cdot \boldsymbol{A}(\boldsymbol{k}) \right) \mod n \\
&= \frac{n}{2\pi} \int_{\partial S_W^2} \mathrm{d}\boldsymbol{s} \cdot \nabla\Phi(\boldsymbol{k}) \mod n \\
&= \frac{n}{2\pi} \Delta\varphi \mod n
\end{aligned}$$

summarizes tables given in:

Fang et al. PRL 108, 266802 (2011), Tsirkin et al., PRB 96, 045102 (2017)

# Outline

1. Local constraint
   Relation between rotation eigenvalues and the chirality

2. Global constraint
   Enforced band exchange by (non)symmorphic symmetry

3. Applications of global and global constraints
   Double Weyl points in TaAs
   Quasi-symmetry-protected quadruple Weyl points
   Fourfold crossing with Chern number $\nu = 5$
   Topological nodal planes
   Chiral nodal lines

# Global constraint I

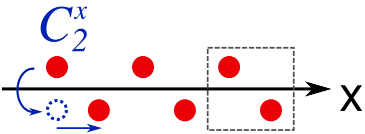


$$(C_n^z(x,y,\tfrac{m}{n}))^n = \pm T(0,0,m) = \pm \exp(imk_z)$$

$$\Longrightarrow \lambda_{C_n} = (\pm 1)^{1/n} \exp\left(i\frac{2\pi p + mk_z}{n}\right)$$

$$\equiv \exp(i\phi(k_z))$$

with band crossings at $\{k_c\}$ $\quad \varphi_b(k_z) = \phi(k_z) + \sum_{k_c \le k_z} \Delta\varphi_{b,c}$

BZ periodicity $\varphi_b(-\pi) = \varphi_b(\pi) \quad \Rightarrow \quad \sum_{c_b} \Delta\varphi_{b,c_b} + 2\pi\frac{m}{n} = 0 \mod 2\pi$

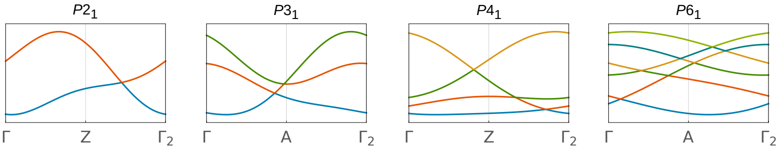

# Global constraint II

If all $c_b$ are two-band crossings:

$$
\begin{aligned}
&b = 1 && \sum_{c_1} \Delta\varphi_{1,c_1} = -2\pi \frac{m}{n} \mod 2\pi \\
&b = 2 && \sum_{c_2} \Delta\varphi_{2,c_2} - \sum_{c_1} \Delta\varphi_{1,c_1} = -2\pi \frac{m}{n} \mod 2\pi \\
& && \Leftrightarrow \sum_{c_2} \Delta\varphi_{2,c_2} = -2 \cdot 2\pi \frac{m}{n} \mod 2\pi \\
&\vdots && \vdots \\
&\text{any } b && \sum_{c_b} \Delta\varphi_{b,c_b} = -b \cdot 2\pi \frac{m}{n} \mod 2\pi.
\end{aligned}
$$

# Outline

1. Local constraint
   Relation between rotation eigenvalues and the chirality

2. Global constraint
   Enforced band exchange by (non)symmorphic symmetry

3. Applications of global and global constraints
   Double Weyl points in TaAs
   Quasi-symmetry-protected quadruple Weyl points
   Fourfold crossing with Chern number $\nu = 5$
   Topological nodal planes
   Chiral nodal lines

# Application to band structures I

Chern number $\nu$ of a band crossing

$$\nu = \Delta\varphi \frac{n}{2\pi} \mod n$$

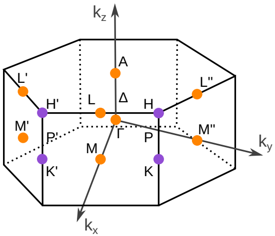


Eigenvalues and Weyl points for SG 144 ($P3_1$)
(simplest arrangement)

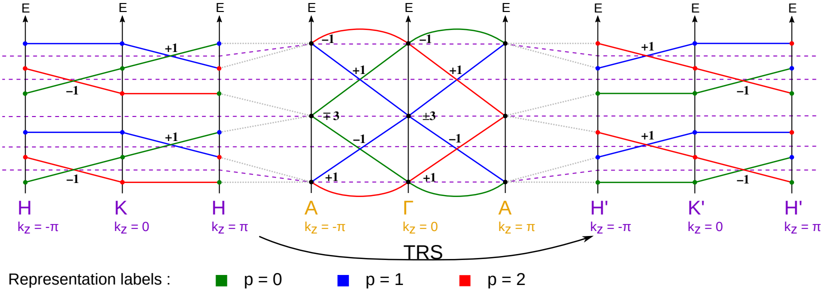


Y.H. Chan, B. Kilic, **M.M.H.**, C.K. Chiu, L.M. Schoop, D.G. Joshi, A.P. Schnyder, (2019). *Physical Review Materials, 3(12), 124204.*

# Application to band structures II

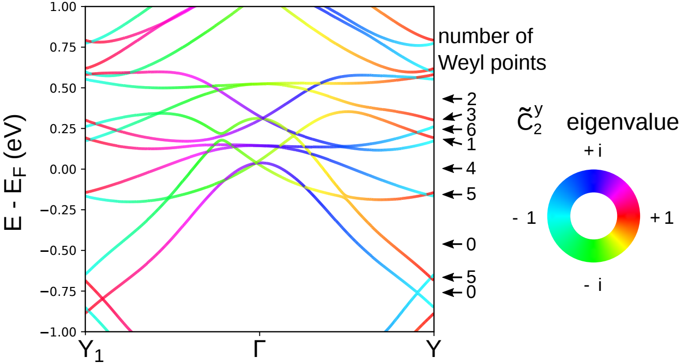


For $C_2^y(0, \frac{1}{2}, \frac{1}{2})$ the global constraint is:

$$\sum_{c_b} \Delta\varphi_{b,c_b} = b \cdot \pi \mod 2\pi$$

every second band exhibits an odd number of Weyl points

M.A. Wilde, M. Dodenhöft, A. Niedermayr, A. Bauer, **M.M.H.**, K. Alpin, A.P. Schnyder, C. Pfleiderer (2021). *Nature, 594(7863), 374-379.*

# Double Weyl points in $TaO_2$

Oxygen deficient $NbO_2$ and (proposed) $TaO_2$

- SG 80 $I4_1$
- $C_4^z T$ creates Kramers pairs at $P$
- At P the only symmetry is $C_2^z$
- $\Delta\varphi = 0, \nu = 0 \mod 2$ : double Weyl point

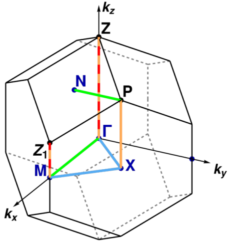


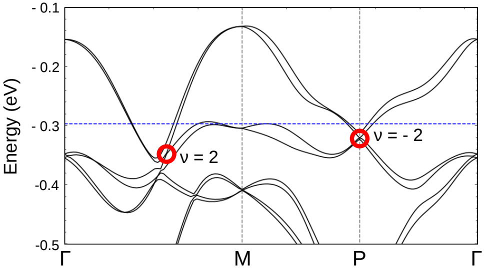


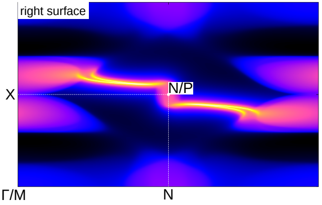

# Quadruple Weyl

Twofold quadruple Weyl points $\nu = \pm 4$ in cubic point groups

T. Zhang, R. Takahashi, C. Fang, S. Murakami, *Physical Review B*, 102, 125148 (2020)

$$H(\boldsymbol{k}) = \left(d_0 + d_1(k_x^2 + k_y^2 + k_z^2)\right)\sigma_0 + a_0 k_x k_y k_z \sigma_z + \begin{pmatrix} 0 & a_1(k_x^2 + k_y^2 \mathrm{e}^{-i2\pi/3} + k_z^2 \mathrm{e}^{-i4\pi/3}) \\ H.C. & 0 \end{pmatrix}$$

for $a_0, a_1 \in \mathbb{R} \Rightarrow H(\boldsymbol{k})$ belongs to point group 432.

Symmetry eigenvalues:

$\lambda_{C_4}$ do not exchange: $\nu = 0 \mod 4$

$\lambda_{C_3}$ exchange: $\nu = \pm 1 \mod 3$

Lowest possible Chern number: $\nu = \pm 4$ (Quadruple Weyl)

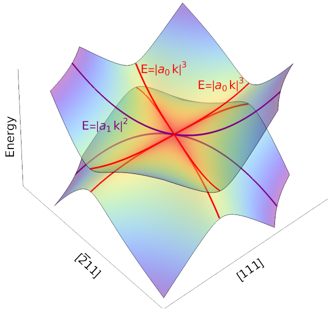

# Quasi-symmetric quadruple Weyl

What happens in a cubic point group without fourfold rotation?
One finds the same Hamiltonian:

$$H(\boldsymbol{k}) = \left(d_0 + d_1(k_x^2 + k_y^2 + k_z^2)\right)\sigma_0 \\ + a_0 k_x k_y k_z \sigma_z + \begin{pmatrix} 0 & a_1(k_x^2 + k_y^2 \mathrm{e}^{-i2\pi/3} + k_z^2 \mathrm{e}^{-i4\pi/3}) \\ H.C. & 0 \end{pmatrix}$$

now with $a_1 \in \mathbb{C}$.

But this is not enough to break the $C_4$ symmetry, needs $k^n$ with $n > 3$
$\rightarrow C_4$ is a quasi-symmetry of the low-energy model.

$$U(C_4^z) = \begin{pmatrix} 0 & \mathrm{e}^{i(\arg(a_1)+2\pi/3)} \\ \mathrm{e}^{-i(\arg(a_1)+2\pi/3)} & 0 \end{pmatrix},$$

$$U(C_4^z)^\dagger H(k_x, k_y, k_z) U(C_4^z) = H(k_y, -k_y, k_z).$$

As before: $\lambda_{U(C_4^z)}$: $\quad \nu = 0 \mod 4 \rightarrow \nu = \pm 4$

# Crossing with chirality $\nu = 5$

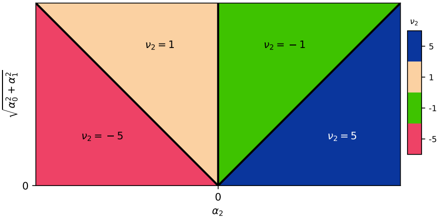


Cubic point group PG 23

- $C_3 : \nu = 1 \mod 3$
  $\rightarrow \nu \in \{\ldots, -5, \quad -2, \quad 1, \quad 4, \ldots\}$
- $C_2 : \nu = 1 \mod 2$
  $\rightarrow \nu \in \{\ldots, -5, -3, -1, 1, 3, 5 \ldots\}$

$\rightarrow$ Lowest possible chiralities $\nu = 1, -5$

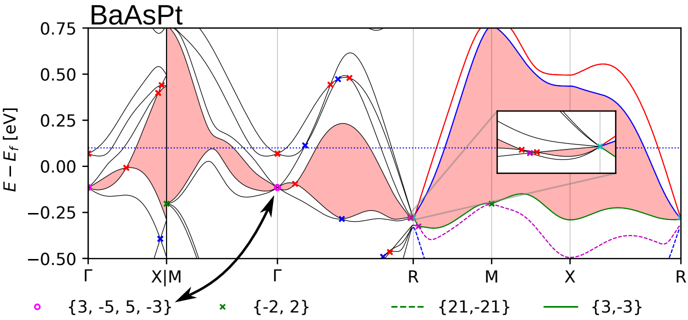

# Nodal planes

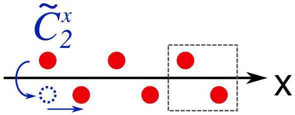


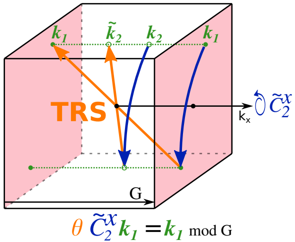


Symmetries:

- two-fold screw rotation $\tilde{C}_2^x$
- time reversal $\theta = i\sigma_y \mathcal{K}$

Kramers theorem applies to $\theta\tilde{C}_2^x$ because

- $(\theta\tilde{C}_2^x)^2 = +T_{(1,0,0)} = e^{ik_x} \underset{\text{at } k_x=\pi}{=} -1$
- invariant planes: $k_x = 0$ and $k_x = \pi$

$(\theta\tilde{C}_2^x)^2 = -1$
$\Rightarrow$ two-fold degenerate plane $k_x = \pi$

M.A. Wilde, M. Dodenhöft, A. Niedermayr, A. Bauer, **M.M.H.**, K. Alpin, A.P. Schnyder, C. Pfleiderer (2021). *Nature, 594(7863), 374-379.*

# Trio of topological nodal planes

Necessary symmetries: Yu, Z. M., et al. (2019). *Physical Review B, 100(4), 041118.*

- $\theta\tilde{C}_2^x$, $\theta\tilde{C}_2^y$, $\theta\tilde{C}_2^z$
  $\Longrightarrow$ three intersecting nodal planes
- $\theta^2 = -1$, single Kramers-Weyl point at $\Gamma$ with $\nu_{\text{Weyl}} = \pm 1$
- Multiplicity of any other Weyl point $> 1$.
  $\Longrightarrow$ nodal planes compensate the Weyl point at $\Gamma$ with $\nu_{\text{NP}} = \mp 1$.

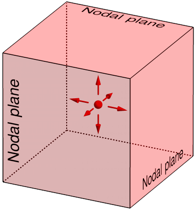


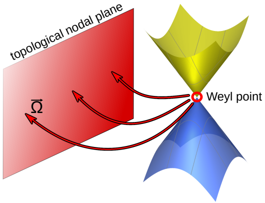


Properties of nodal plane trios:

- No surface states
- Vanishing anomalous Hall effect

# Topological nodal plane duo

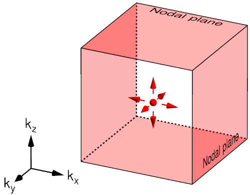


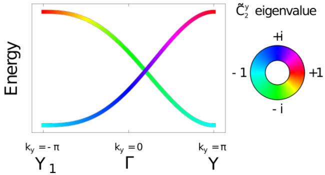


Symmetries:

- $\theta\tilde{C}_2^x$, $\theta\tilde{C}_2^z \Rightarrow$ two nodal planes
- Time-reversal symmetry $\theta$ is broken.
- Two-fold screw rotation $\tilde{C}_2^y$

$\tilde{C}_2^y$ representation:

- $\tilde{C}_2^y$-invariant lines: rotation axes
- $(\tilde{C}_2^y)^2 = T_{(0,1,0)}(i\sigma_y)^2 = -e^{ik_y}$
  $\Rightarrow$ symmetry eigenvalues $\pm ie^{ik_y/2}$

$\Longrightarrow$ uncompensated, odd number of Weyl points

## $\Longrightarrow$ The nodal plane must be topological.

M.A. Wilde, M. Dodenhöft, A. Niedermayr, A. Bauer, **M.M.H.**, K. Alpin, A.P. Schnyder, C. Pfleiderer (2021). *Nature, 594(7863), 374-379.*

# Topological nodal plane duo

Fermi arc:

single Weyl $\rightarrow$ Nodal plane

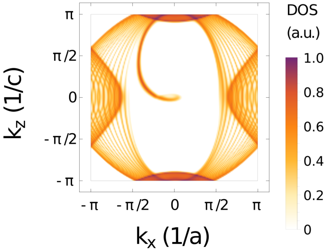


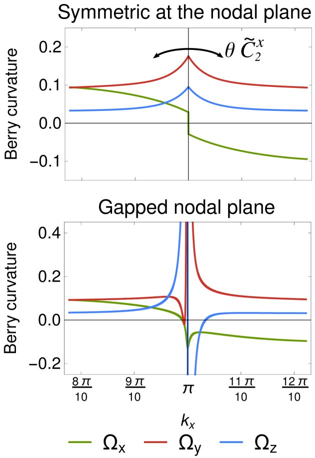


M.A. Wilde, M. Dodenhöft, A. Niedermayr, A. Bauer, **M.M.H.**, K. Alpin, A.P. Schnyder, C. Pfleiderer (2021). *Nature, 594(7863), 374-379.*

# Space groups with nodal planes

**possible** topological nodal plane    **enforced** topological nodal plane

| | | | | | | | | | |
|---|---|---|---|---|---|---|---|---|---|
| Paramagnets | 4.8 [t] | 17.8 [t] | 18.17 [t] | 19.26 [T] | 20.32 [t] | 26.67 | 29.100 | 31.124 | 33.145 |
| | 36.173 | 76.8 [t] | 78.20 [t] | 90.96 [t] | 91.104 [t] | 92.112 [T] | 94.128 [T] | 95.136 [t] | 96.144 [T] |
| | 113.268 | 114.276 | 169.114 [t] | 170.118 [t] | 173.130 [t] | 178.156 [t] | 179.162 [t] | 182.180 [t] | 185.198 |
| | 186.204 | 198.10 [T] | 212.60 [T] | 213.64 [T] | | | | | |
| ~Ferromagnets | 4.9 [t] | 11.54 | 14.79 | 17.10 [t] | 18.18 [t] | 18.19 [t] | 19.27 [T] | 20.34 [t] | 26.68 |
| | 26.69 | 29.101 | 29.102 | 31.125 | 31.126 | MnSi | 33.147 | 36.174 | 36.175 |
| | 51.294 | 51.296 | 52.310 | 52.311 | 53.327 | | 54.342 | 54.344 | 55.357 |
| | 55.358 | 56.369 | 56.370 | 57.382 | 57.383 | 57.384 | 58.397 | 58.398 | 59.409 |
| | 59.410 | 60.422 | 60.423 | 60.424 | 61.436 | 62.446 | 62.447 | 62.448 | 63.463 |
| | 63.464 | 64.475 | 64.476 | 90.98 [t] | 90.99 [t] | 92.114 [T] | 92.115 [T] | 94.130 [T] | 94.131 [t] |
| | 96.146 [T] | 96.147 [T] | 113.269 | 113.271 [t] | $Nd_5Si_4$ | 114.279 [t] | 127.390 | 127.393 | 128.402 |
| | 128.405 | 129.414 | 129.417 | 130.426 | | 135.486 | 135.489 | 136.498 | 136.501 |
| | 137.510 | 137.513 | 138.522 | 138.525 | 169.115 [t] | 170.119 [t] | 173.131 [t] | 176.147 | 178.157 [t] |
| | 178.158 [t] | 179.163 [t] | 179.164 [t] | 182.181 [t] | 182.182 [t] | 185.199 | 185.200 | 186.205 | 186.206 |
| | 193.258 | 193.259 | 194.268 | 194.269 | | | | | |
| ~Antiferromagnets | 3.5 [t] | 3.6 [t] | 4.10 [t] | 16.4 [t] | 16.5 [t] | 16.6 [T] | 17.11 [t] | 17.13 [t] | 17.14 [T] |
| | 17.15 [T] | 18.20 [t] | 18.21 [T] | 18.22 [T] | 18.24 [t] | 19.28 [T] | 19.29 [t] | 20.36 [t] | 21.42 [t] |
| | 21.44 [t] | 25.61 | $CoNb_3S_6$ | 25.65 | 26.71 | 26.72 | 26.76 | 27.82 | 27.85 |
| | 27.86 | 28.94 | | 28.96 | 28.98 | 29.104 | 29.105 | 29.109 | 30.118 |
| | 30.119 | 30.120 | 30.122 | 31.128 | 31.129 | 31.133 | 32.139 | 32.142 | 32.143 |
| | 33.149 | 33.150 | 33.154 | 34.161 | 34.162 | 34.164 | 35.169 | 35.171 | 36.178 |
| | 37.184 | 37.186 | 75.4 [t] | 75.6 [t] | 76.11 [t] | 77.16 [t] | 77.18 [t] | 78.23 [t] | 81.36 [t] |
| | 81.38 [t] | 89.92 [t] | 89.93 [t] | 89.94 [T] | 90.100 [T] | 90.102 [t] | 91.109 [T] | 91.110 [T] | 92.116 [T] |
| | 92.117 [t] | 93.124 [t] | 93.125 [T] | 93.126 [T] | 94.132 [T] | 94.134 [t] | 95.141 [T] | 95.142 [T] | 96.148 [T] |
| | 96.149 [t] | 99.168 | 99.170 | 100.176 | 100.178 | 101.184 | 101.186 | 102.192 | 102.194 |
| | 103.200 | 103.202 | 104.208 | 104.210 | 105.216 | 105.218 | 106.224 | 106.226 | 111.256 |
| | 111.257 | 111.258 | 112.264 | 112.265 | 112.266 | 113.272 | 113.274 | 114.280 | 114.282 |
| | 115.288 | 115.290 | 116.296 | 116.298 | 117.304 | 117.306 | 118.312 | 118.314 | 168.112 [t] |
| | 171.124 [t] | 172.128 [t] | 177.154 [t] | 180.172 [t] | 181.178 [t] | 183.190 | 184.196 | 195.3 [T] | 207.43 [T] |
| | 208.47 [T] | 215.73 | 218.84 | | | | | | |

M.A. Wilde, M. Dodenhöft, A. Niedermayr, A. Bauer, **M.M.H.**, K. Alpin, A.P. Schnyder, C. Pfleiderer (2021). *Nature, 594(7863), 374-379.*

# Nodal plane duo in SG 94

SG 94 $P4_22_12$ with spin-orbit coupling

- Two nodal planes at $k_x = k_y = \pi$
- Along Z-$\Gamma$-Z: hour-glass crossing
- rotation $4_2$: $n = 4, m = 2$

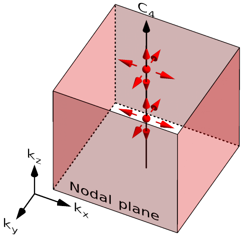


Consider the lowest band $b = 1$ on the fourfold rotation axis:

global constraint: $$\sum_{c_1} \Delta\varphi_{1,c_1} = -m\frac{2\pi}{n} \mod 2\pi$$

Total chirality $\nu_{\text{Z-}\Gamma\text{-Z}}$ on the fourfold rotation axis:

add local constraint: $$\nu_{\text{Z-}\Gamma\text{-Z}} \equiv \sum_{c_1} \nu_{c_1} = \sum_{c_1} \frac{n}{2\pi}\Delta\varphi_{1,c_1} = -m \mod 4$$

$\nu_{\text{Z-}\Gamma\text{-Z}} = 2 \mod 4$ cannot be compensated by generic Weyl points

$\Rightarrow$ The nodal plane duo exhibits a charge of $\nu_{\text{nodal plane}} = -\nu_{\text{Z-}\Gamma\text{-Z}} \neq 0$.

# Application: Chiral nodal lines I

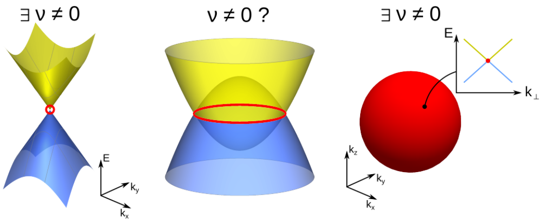


Question: Are chiral nodal lines possible?

- Line protected by mirror symmetry $\rightarrow \nu = 0$
- Can there be a stable line with $\nu \neq n\mathbb{Z}$ enclosing a $C_n$ rotation axis?

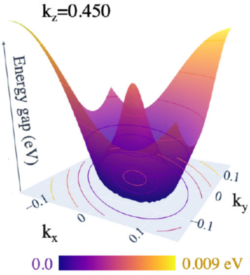


$AgF_3$ - González-Hernández, R., et al PRM 4, 124203 (2020)

# Application: Chiral nodal lines II

Surface *including* line:

$\nu_{\text{line}} + \nu_{\text{axis}} = \Delta\varphi \frac{n}{2\pi} \mod n$

Surface *excluding* line:

$\nu_{\text{axis}} = \Delta\varphi \frac{n}{2\pi} \mod n$

$\Rightarrow \nu_{\text{line}} = 0 \mod n$, thus it cannot be protected by rotation symmetry.

Model of a chiral nodal line:

$$W(\boldsymbol{k}, \epsilon) = \boldsymbol{k} \cdot \boldsymbol{\sigma} + \epsilon\sigma_0$$

$$A(\boldsymbol{k}) = k_z \sigma_1$$

$$H(\boldsymbol{k}) = \begin{pmatrix} W(\boldsymbol{k}, \epsilon) & A(\boldsymbol{k}) \\ A(\boldsymbol{k})^\dagger & W(\boldsymbol{k}, -\epsilon) \end{pmatrix}$$

$$U_{\text{line}} = \frac{1}{\sqrt{5}} \begin{pmatrix} 2 & 0 & 1 & 0 \\ 0 & 2 & 0 & 1 \\ 1 & 0 & -2 & 0 \\ 0 & 1 & 0 & -2 \end{pmatrix}$$

$$[H(\boldsymbol{k}), U_{\text{line}}] = 0$$

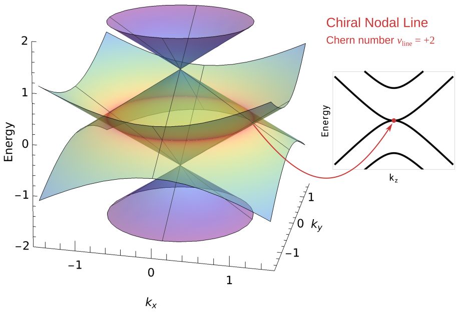

# Summary

- Local constraint
  $\nu = \Delta\varphi \, \frac{n}{2\pi} \mod n$
- Global constraint
  $\sum_{c_b} \Delta\varphi_{b,c_b} = -b \cdot 2\pi \frac{m}{n} \mod 2\pi$
- Applications
  Double Weyl points in TaAs
  Quasi-symmetry-protected quadruple Weyl points
  Crossings with Chern number $\nu = 5$
  Topological nodal planes
  Chiral nodal lines

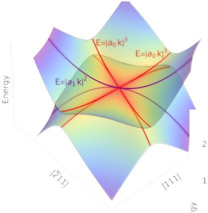


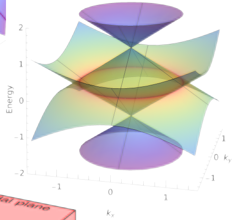


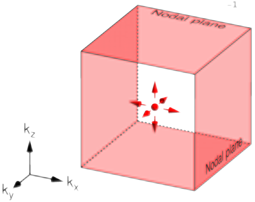

# Summary - Thank you!

- Local constraint
  $\nu = \Delta\varphi \, \frac{n}{2\pi} \mod n$
- Global constraint
  $\sum_{c_b} \Delta\varphi_{b,c_b} = -b \cdot 2\pi \frac{m}{n} \mod 2\pi$
- Applications
  Double Weyl points in TaAs
  Quasi-symmetry-protected quadruple Weyl points
  Crossings with Chern number $\nu = 5$
  Topological nodal planes
  Chiral nodal lines

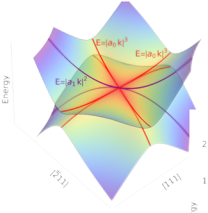


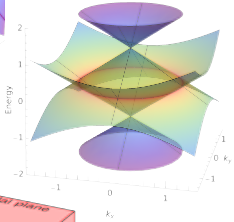


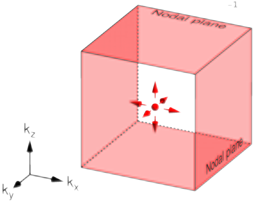

# Topology in a Weyl semimetal

- Chern number $\nu$ : Obstruction to a smooth gauge for eigenstates.
- Wilson loop : Its eigenvalues are the Wannier charge centers.

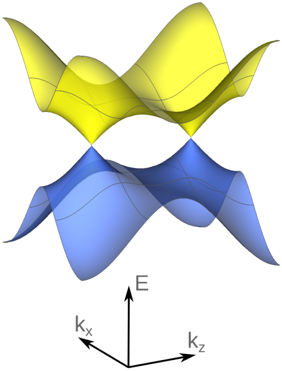


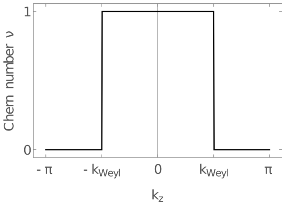


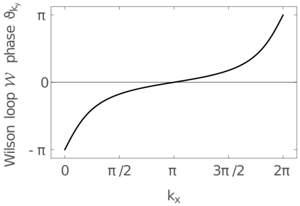

# Band structure of MnSi

Topological nodal planes in ferromagnetic MnSi (mSG 19.27 $P2_1'2_12_1'$)

- Several twofold (WP) and fourfold (FP) Weyl points
- Band degeneracy protected at the Fermi surface: Topological protectorate (TP)

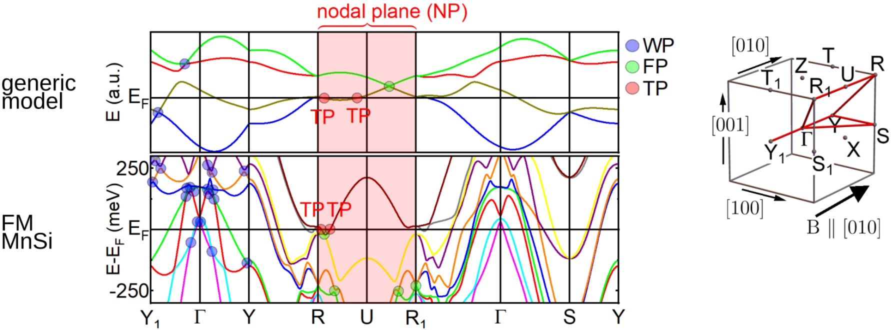


M.A. Wilde, M. Dodenhöft, A. Niedermayr, A. Bauer, **M.M.H.**, K. Alpin, A.P. Schnyder, C. Pfleiderer (2021). *Nature, 594(7863), 374-379.*

# Symmetry eigenvalues in MnSi

Does the picture of the eigenvalue winding argument hold?

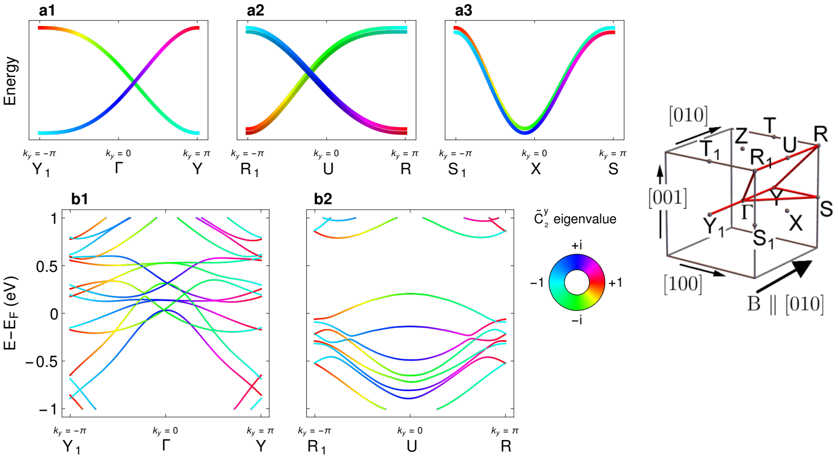


M.A. Wilde, M. Dodenhöft, A. Niedermayr, A. Bauer, **M.M.H.**, K. Alpin, A.P. Schnyder, C. Pfleiderer (2021). *Nature, 594(7863), 374-379.*

# Topological nodal planes in MnSi

Ferromagnetic MnSi (mSG 19.27 $P2_1'2_12_1'$)

Fermi surface sheets

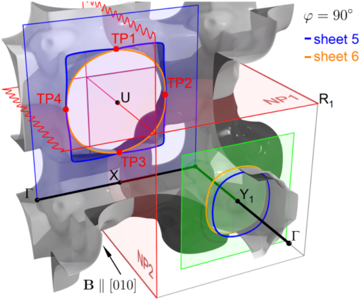


de Haas-van Alphen spectroscopy provides evidence for two gapless nodal planes

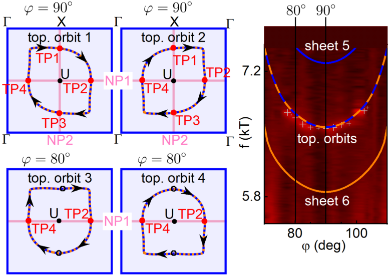


M.A. Wilde, M. Dodenhöft, A. Niedermayr, A. Bauer, **M.M.H.**, K. Alpin, A.P. Schnyder, C. Pfleiderer (2021). *Nature, 594(7863), 374-379.*

# Surface states from DFT for MnSi

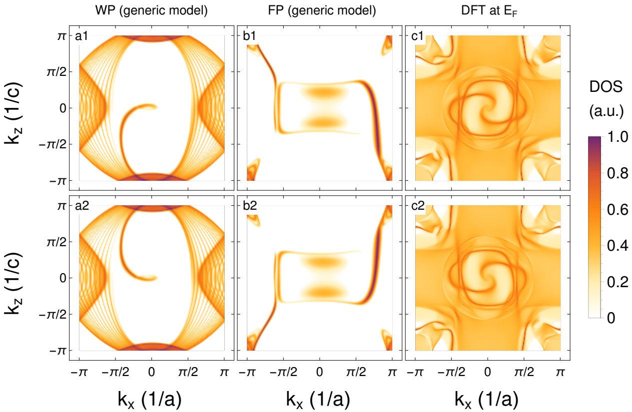


- Generic tight-binding model: Characteristic surface states
- ferromagnetic MnSi: Several overlapping bands, many Weyl points

⇒ Need for simpler systems to study topological nodal planes.


M.A. Wilde, M. Dodenhöft, A. Niedermayr, A. Bauer, **M.M.H.**, K. Alpin, A.P. Schnyder, C. Pfleiderer (2021). *Nature, 594(7863), 374-379.*

# De Haas-van Alphen data

- Oscillations measured using magnetic torque
- Several orbits passing the nodal plane
- Focus on the single frequency $\mathrm{M}_1$.

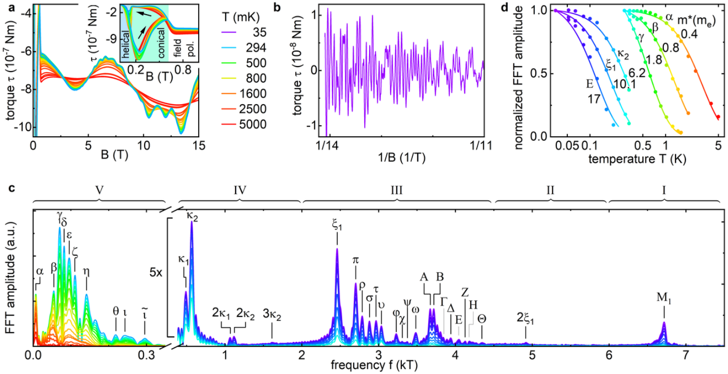


M.A. Wilde, M. Dodenhöft, A. Niedermayr, A. Bauer, **M.M.H.**, K. Alpin, A.P. Schnyder, C. Pfleiderer (2021). *Nature, 594(7863), 374-379*.

# Angle-resolved spectrum

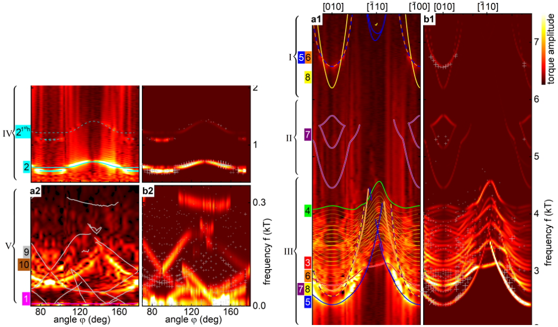

# Band structure for rotated fields

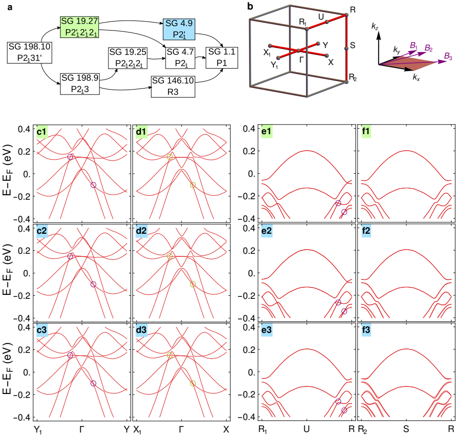

# Berry curvature of the generic model